PV PLANT WITH DISTRIBUTED MPPT FOUNDED ON BATTERIES

La versione pubblicata dall'Editore è reperibile al seguente link (available at):

https://doi.org/10.1016/j.solener.2015.10.017

PV plants with distributed MPPT founded on batteries

Rosario Carbone

University ''Mediterranea" of Reggio Calabria, Via Graziella, loc. Feo di Vito, Reggio Calabria Italy

Abstract This paper introduces and tests a new way of using batteries within a PV plant endowed with a distributed maximum power point tracker (DMPPT). Batteries are used in a distributed framework and they can make possible both the conventional energy storage service and the optimisation of the PV generation. As well known, energy storage is on the basis for solving a lot a problems that are emerging on distribution grids due to the rapid consolidation of the distributed generation. In this paper, it is shown as in PV plants the energy storage availability together with a properly selected value of the rated voltage of batteries can simply avoid generation losses caused by variations on both grid/load operating conditions and also on solar irradiance levels; a further regulation of the rated voltage of batteries, obtained by means of DC/DC converters, can compensate also for generation losses caused by variations on working temperature of PV cells. Finally, batteries used in a distributed framework can guarantee the generation optimisation also in presence of relevant mismatches among PV modules of the whole PV field. In comparison with PV plants with conventional DMPPT (with no energy storage or with a centralized energy storage) the DC voltage at the input terminal of the inverter is very stable and no dangerous overvoltages occur not even in case of strong mismatches among powers generated by different PV modules of a PV field, so the generation of the maximum power is always possible and major costs for batteries acquisition and maintenance can be easily justified. Experiments on a small-power prototype and Pspice numerical simulations are used to demonstrate the usefulness and the practical interest of the proposal.

Keywords: Photovoltaic systems; Distributed generation; Energy storage; Distributed maximum power point trackers

1. Introduction

As well known, electrical power generated by a PV field immediately depends from the solar irradiance level, the temperature of the PV cells and the external grid/load operating conditions. Maximum Power Point Tracking (MPPT) systems (basically, power electronic interfaces) can be utilised to always guarantee the generation of the maximum power compatible with a specific atmospheric exposure of the PV field, for any grid/load condition. Conventionally, in virtue of its rated power, a PV field is divided into a certain number of PV strings; each PV string is composed by a certain number of series-connected PV modules, in order to obtain the best matching with the input operating voltage and the rated power of the inverter. Manufacturing tolerances of PV cells, different orientations of PV modules, partial shadowing of PV modules (caused by any kind of physical obstacle) and so on, are example of causes of mismatching conditions among all the aforementioned series-connected components of a PV string, whose generated current is limited to the lowest value generated by the worse component. In order to limit power mismatching losses in a PV string, its PV modules can be equipped with a bypass diodes; it is connected in anti-parallel at the terminals of a PV module in order to short-circuit it when it is not able to guarantee a generated current of the same level of that generated by the remaining well irradiated PV modules of the same PV string. Even if the bypass diode technique simply alleviates the aforementioned problem, the available power of the by passed modules is completely lost; furthermore, the P–V characteristic of the PV string under mismatches becomes ''multi modal" and this could cause malfunction of the conventional centralized MPPT systems (Shimizu et al., 2003; Silvestre et al., 2009). Distributed Maximum Power Point Tracking (DMPPT) systems have been

introduced to optimise the power generation of a PV field in presence of mismatching phenomena (Walker and Sernia, 2004; Patel and Agarwal, 2008; Femia et al., 2008; Deline et al., 2011; Poshtkouhi et al., 2011; Shmilovitz and Levron, 2012; Alonso et al., 2012; RAMOS-PAJA et al., 2013). Basically, DMPPTs are based on the use of DC/DC converters dedicated to each PV module of a PV string, in order to realise – in a decentralized manner –the MPPT for each PV module; different kind of DMPPTs are based on different kind of useful DC/DC converters (mainly boost, buck, buck-boost, cuck). Theoretically, DMPPTs should optimally extract the sum of the maximum power available at each PV module of a PV string, also in case of mismatching conditions. Undoubtedly, major problems related to DMPPTs are additional costs, additional losses on DC/DC converters and reliability of the resulting more complex circuitry. Nevertheless, an additional issue tied to the use of the aforementioned DMPPTs has been recently introduced and investigated (Chen et al., 2014; Vitelli, 2014). In practice, since the distributed DC/DC converters dedicated to each PV module of the PV string are connected in series at their output ports, the voltage at the output terminals of a single DC/DC converter directly depends on the ratio between its generated power and the whole power generated by the PV string. As a consequence, in case of mismatching conditions, the voltage at the output terminals of the DC/DC converter providing the higher power can become very large so causing dangerous voltage stresses on its components; to avoid destruction of converter components, a voltage limitation technique must be implemented or the MPPT function must be temporary stopped, and this immediately causes relevant reductions on the whole generated power. In order to contain this particular kind of additional losses on the whole power generated by a PV string endowed by a DMPPT, in (Vitelli, 2014) it is proposed to add a central MPPT on the PV string inverter, in order to optimally control the values of its input voltage (also, the whole output voltage of the PV string); the higher the rating of the devices of the distributed DC/DC converters the higher the performances that can be obtained and/or the wider the amplitude of the optimal operating range of the inverter input voltage. Nevertheless, an additional circuitry (and costs) is needed without totally avoiding generating losses caused by mismatches. Furthermore, an other important consideration must be taken into account in looking for the optimal architecture and/or control logic of MPPTs for photovoltaic plants, as explained in the follow. In this last years, grid-connected generation plants from renewable have registered a great diffusion and – in turn – HV, MV and LV transmission and distribution grids have registered serious and remarkable integration problems, mainly because they have been historically designed and managed as passive systems, i.e. without injection of active power by the end-users; the connection to the grid of large amounts of intermittent renewable energy sources has proved of causing voltage rise along the feeders (especially in LV grids) and/or an increase in harmonic content at the PCCs and/or an increase in the voltage unbalance and so on. In order to cope with the aforementioned problems and to allow for an effective integration of distributed generation into power grids, owners of distributed generation plants have to strictly interact with grid Operators and, some technical constraints for their plants are imperative. With some details, a modern grid-connected distributed generation plant must be able to stay connected with the grid only if the PCC voltage and frequency are within a certain range of its nominal values, avoid (or limit) the injection of DC current components, participate to the reactive power flow into the grid, avoid the islanding condition in case of voltage dips, control the active power injected into the grid and so on. At the international level, this issue is now well represented within contents of the standards IEEE 1547 (2003), IEEE 1547.3 (2007), Network Codes of ENTSO-E (http:// networkcodes.entsoe.eu/) and the regulation (EC) N. 714/2009 of the European Parliament (Regulation (EC), 2009); also at the Italian level, regulation of distributed energy generators has been recently revised, with different constraints depending on the connection voltage levels (the TERNA Network Code (TERNA, 2005) for the HV level, the CEI 0-16 (CEI 0-16, 2012) for the MV level and the CEI 0-21 (CEI 0-21, 2014) for the LV level). In this emerging contest, remote control and/or limitations, operated – de facto – by grid operators, even on the active power injectable by grid-connected PV plants, can immediately frustrate the basic function of conventional MPPTs with no energy storage, regardless their typology and/or their control algorithms and/or the robustness of their constituent devices. Now, is strengthening more and more the view that one way for consolidating the spread of distributed generation from renewable and, also, for maintaining the intrinsic value of MPPTs, is

that of introducing energy storage systems also in grid-connected PV plants (Carbone, 2009a, 2010, 2011; Edrington et al., 2010; Sun et al., 2011; Du and Lu, 2011; Carbone and Tomaselli, 2012; Bong-Yeon Choi et al., 2012; Ali et al., 2012; Burgio et al., 2013; Kim et al., 2013; Jabalameli et al., 2013; Beltran et al., 2013). In recent years, a lot of papers have been published in the specialised literature to discuss about the usefulness of energy storage systems in modern distribution grids, especially in presence of distributed generation systems from renewable (PV plants, wind farms, fuel cells, high-efficiency co-generation systems, ...). Regardless the technology of the used energy storage systems (batteries, super-capacitors, super-magnetics, flywheels, pumped hydro, compressed air, hydrogen, ...), the main outcome of all these studies is that energy storage is on the basis of the achievement of very important and valuable ancillary services, able to significantly improve reliability, availability and power quality of modern distribution grids. In this paper, a battery-based energy storage system is considered in grid-connected PV plants; differently from other well established solutions, batteries are utilised in a decentralized manner as base for coping with the additional task of implementing a reliable and efficient distributed MPPT system. In a nutshell, once the PV field has been partitioned in a certain number of PV strings, in virtue of its power and solar exposure, each PV string is – in turn – partitioned in a certain number of sub PV strings, whose PV modules are characterised, as much as possible, by a uniform exposure to atmospheric agents. Then, for each sub PV string, a properly designed/matched battery pack is introduced; regardless to its capacity, that not immediately affect generation properties of the sub PV string, its nominal voltage is chosen – as close as possible – to the voltage at the maximum power generated by the sub PV string under actual operating conditions; this already guarantees the implementation of a first order passive MPPT, for each sub PV string (Carbone, 2009b). In order to compensate for variations of the irradiance level and, mostly, of the working temperature of PV cells, the battery pack is connected at the output terminals of the sub PV string via a simple boost-type DC/DC converter, so implementing a more accurate second order active MPPT function. Once each sub PV string has been endowed with its battery-packs, sub PV strings can be connected in series among them to supply the PV string inverter. In the following, the proposed architecture of the PV plant and the designing of each sub PV string with its battery pack and its DC/DC converter are described with some more details; the criterion for selecting the rated voltage of the battery-packs will be outlined while – at this stage – no specific emphasis will be given to the criterion for selecting the capacity value of batteries, because it is strongly dependent from specific characteristics of the PV plant and from the mismatching scenario that has to be coped with (small-power or high-power PV plant, random or periodical mismatches, short-time or long-time mismatches, ...). An all inclusive Pspice numerical model of a PV plant is also introduced; firstly, it is well setted with the help of a ‘‘basic” small-power lab prototypes, constituted by a mini PV module, a DC/DC converter and a battery pack; then, it is simply extended to a more complex and interesting 3 kWp PV plant case-study endowed with a distributed MPPT. The analyses are intended to demonstrate the usefulness of the proposed battery-based PV plant architecture also in case of some critical operating conditions.

2. The proposed architecture

Fundamentals on the proposed idea can be firstly appreciated with the help of Figs. 1 and 2. In practice, the PV field is firstly partitioned into a proper number of PV strings; then, for each PV string, the PV modules characterised by a very reduced probability of mismatches among them are identified and grouped in a certain number of sub PV strings; this last, together with its DC/DC converter and its battery-pack, constitutes – de facto – the here called ‘‘battery-based PV generator”. As shown in Fig. 2, in the i-th battery-based PV generator the sub PV string is connected to its battery-pack via a boost-type DC/DC converter. In this way, once the rated voltage of the battery-pack, Vbatt, has been properly matched with its sub PV string – mainly by taking into account its actual operating characteristics – it can be further regulated by controlling the duty-cycle value, k, of the DC/DC converter, in order to obtain a working voltage, Vpv, at the sub PV string terminals able to make always possible the generation of its maximum power, regardless of the irradiance level, the

temperature of the PV cells and the external grid/load operating conditions. In this sense, the first step of properly matching the rated voltage of the battery pack with the operating characteristics of the sub PV string (although within limits imposed by commercial availability of batteries) can be considered as a ‘‘first order” passive MPPT setting, while the more accurate adjustment of this voltage operated by the DC/DC converter can be considered as a ‘‘second order” active MPPT operation. The boost type DC/DC converter is very simple and inexpensive (it is simply based on few additional components); it has to guarantee only a small regulation for Vpv, starting from the properly selected Vbatt value; then, very small conduction losses are expected. The more the inductance value of L is high, the more the switch Q can be, also, operated at low switching frequencies for containing also switching losses. An additional advantage of the boost-type DC/DC converter is that its inductor, L, results in series with the sub PV string so guaranteeing an almost continuous generated current; as a consequence, an additional capacitor at the sub PV string terminals is not strictly needed. Differently from conventional architectures with distributed MPPT but with no distributed batteries, in the proposed architecture, even if a PV string is constituted by a number of sub PV strings in series at their output terminals, the DC/DC converters are not connected in series among them. In fact (see Fig. 2), the output current of the PV string, io, injected into the grid or given to the load and also common to all the battery-based PV generators of the same PV string, is the sum of the DC–DC converter current, iD and the battery current, ibatt; this means that, if one (ore more) sub PV string is not well irradiated as the other ones, thanks to its own battery-pack, its associated PV generator can generate (temporarily, within the limits of the capacity of its battery pack), the same current io generated by well irradiated sub PV strings. In this way, each sub PV string can always generate its own maximum available power, regardless of the grid/load operating conditions, the ratio among the power generated by each sub PV string and the whole power generated by the PV string, the value of the whole input inverter voltage and so on. Furthermore, the whole output voltage of the PV string (that is also the input voltage of the inverter) is quite constant and this should guarantee the maximum efficiency for the inverter together with no dangerous overvoltages on the DC–DC converter components, also in presence of critical mismatching conditions among the sub PV strings.

3. Setting a Pspice numerical model on a single battery-based PV generator

Developing and testing an all inclusive prototype of a newly introduced circuitry is, of course, a very good thing for analysing and evaluating its performances and/or effectiveness. Nevertheless, in case of very complex architectures or circuitries, whose behaviour and performances are strongly dependent also from a lot of boundary conditions, as is the case of a PV plant with a distributed MPPT, the setup and the use of a reliable and all inclusive numerical model can result a good alternative to a complex prototype. If well setted, an inclusive numerical model can be very practical and useful; furthermore, it can give evidence of some phenomena that are difficult to forecast and/or to analyse theoretically or exclusively with campaigns of onsite measurements and/or on an inclusive lab prototype. For this reason, in the following, an inclusive Pspice numerical model, to be used for analysing the architecture proposed in Section 2, is introduced; for the sake of brevity, some more deep details on the construction process of this model are not reported here and they can be found in (Carbone et al., 2014). Firstly the Pspice numerical model is well setted having in mind only a single battery-based PV generator (Fig. 2); Fig. 1. Architecture of the proposed PV plant with the battery-based distributed MPPT. Fig. 2. Electrical scheme of the i-th battery-based PV generator with its MPPT. R. Carbone / Solar Energy 122 (2015) 910–923 913 then, in Section 4, it is simply extended to the more complex and interesting architecture of Fig. 1. In Section 3.1 the numerical model of a generic commercial PV cell is introduced and experimentally setted. In Section 3.2 the inclusion into Pspice of both the numerical model of a boost-type DC/DC converter with its control logic and the numerical model of a battery pack is discussed and the numerical model for a whole single battery-based PV generator is picked out. In Section 3.3 a home-made low-power prototype of a battery-based PV generator is presented; it includes an artificial irradiance system, a mini PV module, a boost-type DC/DC converter with its control, a battery pack and a

variable resistive load. Measurements on this lab prototype are utilised for a good setting of the Pspice numerical model identified in Section 3.2. To obtain this goal, two different campaigns of measurements and simulations are utilised; ‘‘short-time” measurements and simulations are used to give evidence of the goodness of the Pspice numerical model in evaluating instantaneous powers under different operating conditions; ‘‘long-time” measurements and simulations are used to give evidence of the goodness of the Pspice numerical model in reproducing the behaviour of batteries together with their effects on the generation ability of the lab PV module. Once the Pspice numerical model of a generic battery based PV generator is well setted with the help of experimental tests on the lab prototype, the analysis presented in Section 4 is solely based on the use of the Pspice numerical model, that is simply extended to a more complex and interesting 3 kWp PV plant case-study. This last analysis is fully intended to show the usefulness of the proposed battery-based architecture and to underline its advantages with respect to other architectures based on conventional (with no batteries) distributed MPPT.

3.1. Setting a Pspice model for a PV cell (or a module or a string)

The exponential double-diode model of Fig. 3 together with Eq. (1), which take into account some intrinsic non ideality factors typical of photovoltaic devices, are here used to reproduce the I–V characteristic of a PV cell,

$$I = I_{ph} - I_{01}\left(e^{\frac{V+IR_S}{nV_T}} - 1\right) - I_{02}\left(e^{\frac{V+IR_S}{mV_T}} - 1\right) - \frac{V + IR_S}{R_{Sh}}, \qquad (1)$$

where as well known, I is the PV cell terminal current, V is the PV cell terminal voltage, Iph is the photo-generated current, linearly depending on the solar irradiance, I_{01} is the dark saturation current due to recombination in the quasi neutral region (diffusion), I_{02} is the dark saturation current due to recombination in the space charge region, n is the non-ideality factor of the first diode, m is the non-ideality factor of the second diode, Rs is the series resistance, Rsh is the shunt resistance and VT is the thermal voltage.

The PV cell model parameters depend on environmental conditions and on the materials the cell is made of; their values can be derived by comparison to experimental I–V characteristic curves furnished by manufactures. In the SPICE environment, our model uses voltage controlled current generators instead of diodes, because they allow to implement more effectively the analytical equations of the model for a more efficient computation. In this work we considered 6’’x 6’’ polycrystalline silicon cells and the following values of the characteristic parameters have been identified in Standard Test Condition (25 °C, 1000 W/m^2): I_{01} = 4.1x10^{-11} A, I_{02} = 2.8x10^{-7} A, Iph = 8.17 A, Rs =3mΩ, Rsh = 4 Ω. To allow the model to simulate the real behaviour of the PV cell under variable atmospheric conditions, the dependence of temperature and irradiance is also introduced. The simulation model considers the value of the irradiance (W/m^2) and the temperature (°C) at the cell surface, and the photo-generated current is:

$$I_{ph} = I_{ph,ref}(G/G_{ref}) + \alpha(\mathrm{T} - \mathrm{T}_{ref}), \qquad (2)$$

where G_{ref}, $I_{ph,ref}$, T_{ref} are, respectively, the irradiance, the photo-generated current and the temperature in reference conditions and a is the experimental current temperature coefficient (3.26 mA/°C). For the two dark saturation currents the temperature dependence is introduced with the following equations obtained through an exponential interpolation of the I_{01} and I_{02} values extracted at different temperatures:

$$I_{01} = 4.1 \times 10^{-12} \cdot e^{0.1658 \cdot \mathrm{T}}, \qquad (3)$$

$$I_{02} = 2.8 \times 10^{-7} \cdot e^{0.1256 \cdot \mathrm{T}}. \qquad (4)$$

The PV cells were characterised with a QuickSun 120CA Cell Solar Simulator reproducing the solar spectrum, whereas a hot air gun and a thermal imaging camera have been used to regulate the cell temperature; the results are fully reported in (Carbone et al., 2014). Once the numerical model of a PV cell has been setted, a PV module (or a PV string) can be simulated by simply placing in series several solar cells and this can be accomplished by simply multiplying some parameters of the PV cell for the number, Ns, of the PV cell to be put in series; again, for some more details please refer to (Carbone et al., 2014).

3.2. Including a Pspice model of a boost-type DC/DC converter endowed with a battery pack

With reference to Fig. 2, also a Pspice numerical model of the boost type DC/DC converter has to be setted. Basically, this is simply achieved by using conventional libraries already present into the Pspice environment, that are known to be able to properly model an inductor, L, a power switch, Q, together with its control logic, a diode, D, and the also a battery-pack. An additional resistor (Rs) was also introduced in series with the inductor, to simulate both the internal resistance of the inductor and resistances of connections among circuit components. For the sake of simplicity, the PV string inverter was simply modelled with a variable resistive load, without affecting the generality of our conclusive considerations. Obviously, the battery model is crucial for the subsequent numerical analysis; far from being a simple ideal constant voltage source, the Pspice numerical battery model used in this paper is fully described in Castaner and Silvestre (2002). This numerical model is able to reproduce variations of the voltage at the battery terminals (Vbatt), starting from its fixed open circuit value (V_{oc}) and by taking into account charging/discharging battery current (I_{batt}), the assigned battery capacity value (Ah) or the maximum value of the battery state of charge (S_{OCm}, in Wh), the initial value of the battery state of charge (SOC) and the internal charge/discharge battery resistance (R). In practice, the electrical battery model is composed of a voltage source (V) in series with a resistor (R), which values depend on the battery operation mode at a given time. This battery model can be also adjusted to improve Pspice simulation results of PV systems involving any given type of commercial battery, either by taking into account the data provided by the manufacturer or by deriving empirically the values of the model parameters. Remembering that most PV systems include overcharge and undercharge protections to avoid a reduced battery life, only the two main modes of operation (charge and discharge) are modelled. This means that overcharge and undercharge operation modes of battery are not modelled; also the effects of the battery working temperature have not been considered, although they could be easily included (Castaner et al., 1995). In order to prove the validity of the inclusive Pspice numerical model of a single battery-based PV generator (Fig. 2), a number of simulations are performed under different operating conditions and the results are compared with the results of laboratory measurements performed on a home-made low-power prototype whose electrical scheme and some pictures are reported, respectively, in Figs. 4 and 5. The mini PV module (constituted by six of the 6''x 6'' polycrystalline silicon cells already characterised in Section 3.1) has been irradiated artificially by means of a couple of projectors endowed with halogen 500 W lamps; irradiance levels variable from 150 W/m^2 to 600 W/m^2 can be obtained by simply regulating the distance of the projectors from the PV module; with the same procedure and with the help of a small air fan a variable working temperature of the PV cells, from 20 °C to 60 °C, can be also obtained. With the help of some lab measurements, a value of 0.3 Ω has been estimated for the parasitic resistor, Rs, emulating both the internal resistance of the inductor and resistances of connections among circuit components. Fig. 6 shows some details of the implemented Pspice circuitry. The results of measurements and simulations together with some discussion about their comparisons and capabilities of the battery pack are reported in next section 3.3.

3.3. Measurements and numerical simulations

Firstly, some ''short-time" (just few seconds) measurements and simulations have been performed. Obviously, during these tests no significant charging/discharging effects on the battery-pack have been obtained and evidenced, so they have to be intended only for demonstrating the goodness of the Pspice numerical model in evaluating instantaneous powers generated by the lab prototype, under different

working conditions (variations of the irradiance, of the temperature and of the load condition). In Fig. 7 the measured (left) and simulated (right) waveforms of the Q gating signal, Vpulse, and the current generated by the mini PV module, are reported for a first qualitative comparison. For a more complete comparison, in Fig. 8 and Table 1 some additional results, obtained under variable working conditions, are further reported. A good accordance between measurements and simulations is always evident, that is to say the Pspice numerical model has a good modelling accuracy; furthermore, the maximum available power can be always generated by the mini PV module, also under critical load conditions (far from the optimal value) and variable atmospheric conditions, by simply controlling the duty-cycle, k, of the DC/DC converter. Obviously, during short-time measurements and simulations, voltage across the battery-pack does not undergo substantial changes and the behaviour/properties of the battery numerical model cannot be fully underlined. For this reason, also ‘‘long-time” (some thousands of seconds) measurements and simulations have been performed. During these tests, in order to avoid very long computational times in using the Pspice, the DC/DC converter of Fig. 4 was kept always off (that is to say the switch Q was kept always open); this is also for showing as the battery pack can act as an effective ‘‘first order” passive MPPT, if its rated voltage is properly matched by taking into account operating characteristics of the circuit under consideration. In this sense, the battery-based circuits have been always compared with the same circuits with no battery-pack (the battery-pack was simply switched off). In practice, two different ‘‘long-time” tests have been performed referring to both a wrong and a right criterion of matching the battery-pack to its sub PV string. In the first test, the rated voltage of the battery-pack has been designed by taking into account only the theoretical open circuit voltage of the PV mini-module under standard conditions (about 3.3 V) and the commercial availability of batteries; thus, a battery pack with 2.4 V of rated voltage (about 2.6 V of open circuit voltage) has been utilised. Furthermore, to guarantee power continuity at a load of about 10 W for 1 h (hypothesis of medium-time outage of PV generation) a fully charged (SOC = 1) battery pack with 4.2 A h of capacity has been used. Please note that, any other hypothesis on possible time-outages of the PV generation (that could be of practical interest) together with any other possible load condition immediately affects the selection of the capacity (and additional cost) of the battery-pack while it does not affect the selection of its rated voltage, that here is considered the most interesting question to be coped with. Critical absence of solar irradiance (0 W/m2 for a very long time) together with a low availability of solar irradiance (280 W/m2) have been both considered; a ‘‘medium power” load condition together with the optimal load condition have been also played. With the help of an air fan, the temperature of PV cells was always maintained at about 25 °C. Fig. 9 refers to the critical very long time outage of PV generation at a medium power load condition (Rload = 0.76 Ω); obviously, any power is furnished to the load when the battery is switched off (battery-OFF), while with the battery-ON the load is supplied with a mean power of about 5.5 W for almost 5000 s. A good accordance is registered between simulated and experimental results; nevertheless, because of inherent modelling limits, at the undercharge stage the battery numerical model does not longer provide a satisfactory response, so these operating conditions should be avoided in utilising the numerical model. Fig. 10 refers to a low irradiance level of about 280 W/m2 at the optimal load condition (at this irradiance level it coincides with the aforementioned medium load Rload = 0.76 Ω); in the circuit with the battery-OFF, the PV module generates the maximum available power of about 5.5 W while in the circuit with the battery-ON the PV module generates only 2.6 W so showing a very negative effect of this ‘‘wrong” designed 2.4 V battery-pack. This is because the rated voltage of the battery pack has been chosen too high; in fact, during aforementioned operating condition, a voltage of about 3.1 V has been registered at the terminals of the PV module and this is higher than its 2.6 V maximum power voltage. Anyway, the battery-pack is able to supplies the load with an initial power of 6.5 W, fully discharging in about 7000 s. When battery is discharging a little higher power is generated by the PV module due to the lowering of the battery voltage; nevertheless, when battery undercharges PV generation is completely lost. In the second test, a more accurate selection of the rated voltage of the battery-pack has been operated; in fact, parasitic voltage drops on circuit components interposed between the PV mini-module and the battery pack (inductor, diode and connection of components) have been additionally taken into account and experimentally estimated and a battery pack

with a reduced 1.2 V of rated voltage (about 1.37 V of open circuit voltage) has been chosen; for coping for the same hypothesis of 1 h outage of the PV generation at a 10 W load condition, a fully charged (SOC = 1) battery-pack with 8.4 A h of capacity has been utilised. Again, aforementioned operating conditions with critical very long time outage of PV generation and with a low availability of solar irradiance (280 W/m2) have been both considered. Optimal and non-optimal load conditions have been also played. With the help of an air fan, the working temperature of PV cells was always maintained at about 25 °C. Fig. 11 refers to a critical very long time outage of PV generation at a medium power load condition (Rload = 0.23 Ω); obviously, any power is furnished to the load by the circuit with the battery-OFF while the circuit with the battery-ON is able to supply the load with about 4 W for almost 7000 s. A good accordance is registered between simulated and experimental results except that at the undercharge phase. An operating condition characterised by a low irradiance level of about 280 W/m2 at the optimal load condition (Rload = 0.76 Ω) has been also considered; in the circuit with the battery-OFF, the PV module generates the maximum available power of about 5.5 W while in the circuit with the battery-ON the PV module generates about 5.3 W so showing that a ''rightly" designed battery-pack does not introduce significant disturbances on generation capability of the PV module under the optimal load condition; furthermore, the battery-pack is also able to supplies the load for a long time with a power of about 2.5 W different from the generated one. A good accordance is registered between simulation and measurements. Additionally, Fig. 12 refers to a low irradiance level of about 280 W/m^2 at a non optimal load condition (Rload = 0.2 Ω); in the circuit with the battery-OFF, the PV module generates a power of about 3.8 W (lower than the maximum available power) while in the circuit with the battery-ON the PV module again generates 5.3 W so showing that a ''rightly" designed battery-pack can also act as a passive ''first order" MPPT guaranteeing the generation of about the maximum available power also under non optimal load conditions. However, in virtue of its limited capacity value and because in this case it has to supply the load with a power higher than the generated one (about 6.5 W), the battery-pack allows the generation of the maximum power (together with the load supply) only for a limited time of about 9000 s. Finally, Fig. 13 shows as, at a certain temperature (e.g. 25 °C) and at a certain irradiance level (e.g. 280 W/m^2), a rightly designed battery pack can guarantee the PV generation of the maximum available power also for any non optimal load condition while this is not if batteries are switched-OFF. Nevertheless, the battery-pack cannot guarantee the generation of the maximum power if the temperature of PV cells varies significantly; for this reason, a ''second order" active MPPT, based on the activation of boost-type DC/DC converter, is advisable.

4. Numerical analyses on a 3 kWp case-study PV plant with distributed MPPT

Once the Pspice numerical model of a single battery-based PV generator has been setted, it can be simply extended to a more complex architecture (Carbone et al., 2014); thus, in the following it is utilised for analysing a more practical and interesting case-study of residential PV plant with about 3 kWp endowed with a distributed MPPT; the analysis is intended to show advantages of the proposed battery-based architecture with respect to conventional (with no batteries) distributed MPPTs. For the sake of brevity and for avoiding very long computational times, only short-time simulations are performed, for estimating instantaneous (or short-time) voltages and powers on different circuitries, under different operating conditions.

The case-study PV field is based on 12 commercial PV modules with 240 Wp of rated power, under standard conditions (1000 W/m2 of irradiance, G, and 25 °C of temperature, Tc). Each PV module is based on 60 series-connected PV cells, with about 4 Wp of rated power (PV cells already introduced in Section 3.1). For the sake of simplicity and without any loss of generality, only a single PV string, based on all the 12 PV modules, is hypothesised. The PV string is partitioned into 3 sub PV strings; each sub PV string is based on 4 series-connected PV modules, that are hypothesised to be always subject to identical atmospheric conditions; each sub PV string is also endowed by its proper DC/DC boost-type converter, for maximum power tracking. The three sub PV strings are connected in series at their output terminals. In order to

compare performances of the proposed architecture with those of a conventional architecture both referred to a PV plant endowed by a distributed MPPT, two different circuitries are simulated by means of the Pspice numerical model; in the first one (the conventional) at the output terminals of each DC/DC converter a capacitor is – conventionally – attached; in the second one (the proposed) the aforementioned capacitor is substituted by means of a properly designed battery-pack. Without any loss of generality, the central inverter and the grid/load are modelled by an equivalent variable resistor, to simulate both optimal (central MPPT ON) and non optimal (central MPPT OFF) load/network operating conditions. For the sake of brevity, only the Pspice circuitry of the proposed architecture is reported in Fig. 14. For the proposed architecture, taking into account the operating characteristics of each sub PV string (4 series connected 250 Wp PV modules), a lead acid valve-regulated battery pack with 144 V of rated voltage has been selected. About the selection of the capacity of the battery pack, hypothesising that our main objective is simply that of compensating for possible short-time (just few minutes) atmospheric mismatches among the 3 sub PV strings (also avoiding undercharge of batteries), a capacity value of 12 Ah has been considered more than enough. For the architecture based on the conventional distributed MPPT, a 470 uF commercial aluminium electrolytic capacitor has been utilised for substituting the battery-packs evidenced in Fig. 14. To enable the highlighting of a critical (probably, the most interesting) issue related to the implementation of the conventional architecture, that is to say possible dangerous overvoltages on circuit components, a generic Dbreak Pspice diode model with no peak reverse voltage limitation has been now used for both circuitries, instead of a commercial diode with a limited peak reverse voltage. In next Section 4.1, advantages of the proposed battery based architecture with respect to a conventional architecture with no batteries are firstly underlined referring to operating conditions characterised by the absence of any kind of mismatches among the 3 sub PV strings, having played significant variations on grid/load operating conditions. In Section 4.2, operating conditions characterised by significant mismatches among sub PV string irradiance values are then considered.

4.1. Numerical analyses in case of balanced irradiance levels

Standard atmospheric conditions (1000 W/m^2 of irradiance level and 25 °C of temperature) are taken into consideration for all the 3 sub PV strings of Fig. 14. In Fig. 15, the values of the maximum power, Pg, generated by the whole PV string, under different (and non optimal) values of the grid/load equivalent resistance, Rload, are reported, for both the proposed and the conventional architecture; in Fig. 16, the values of the whole output voltages, V_0 (at the terminals of the Rload), are also reported. Figs. 15 and 16 evidence as the proposed architecture shows the ability to always generate the maximum power (about 2.5 kW) independently from the grid/load operating condition and with an output voltage almost constant and within the range of the rated value of the battery-packs. This means that DC/DC converters can be operated with constant e low value duty-cycles, so obtaining also a very low conversion power losses (in our case, losses less than 10 W have been registered). On the contrary (Fig. 15), the conventional architecture generates the maximum power only for values of the equivalent grid/load resistance above a certain limit (in our case about 50 Ω). Anyhow, the output voltage (Fig. 16) strongly depends on the grid/load operating conditions, arriving to become even potentially destructive for some circuitry components; furthermore, to obtain the maximum available power, duty-cycle values of DC/DC converters have to be very variable, reaching, at high values of Rload, values greater than 50% that cause high power conversion losses (in our case, losses higher than 60 W have been registered).

4.2. Numerical analyses in presence of mismatches

A case-study characterised by significant mismatches, in terms of different irradiance levels among the 3 sub PV strings, is now considered; in particular, a 25 °C standard value of the temperature for all the sub PV strings, a 1000 W/m^2 value for the irradiance level for the 1-th sub PV string (upper side in Fig. 14) and a

200 W/m^2 value for the irradiance level of both the 2-th and 3-th sub PV strings, are hypothesised. A number of simulations have been operated, referring to both the conventional and the proposed architecture, for evaluating the maximum power generated by each sub PV string, Pj, together with the total one, Pg, for different values of Rload. The results in terms of Pg are reported in Fig. 17; the values of the whole output voltage, V_0, are reported in Fig. 18 and, finally, in Fig. 19, the values of the output voltages of each-PV string, $V_{0,j\text{-}th}$, are also reported, but only referring to the conventional architecture. As shown in Figs. 17 and 18, also in this case the proposed architecture is able to generate the maximum available power (about 1100 W), for any grid/load operating condition and with an almost constant output voltage, V_0. On the contrary, the conventional architecture seems able the generate the maximum power only starting from certain high values of Rload (Fig. 17); in particular the lower the value of Rload the lower the partial power generated by the less irradiated sub PV strings and under certain values of Rload, power generated by the less irradiated sub PV strings becomes null (in fact, their output voltage becomes null); even, this contribution could become negative, if a bypass diode is not installed at the output terminals of each sub PV string (in fact, their output voltage could also become negative). That said, it is evident that, for the conventional architecture, a central inverter is strictly needed for allowing the generation of the maximum possible power by controlling the equivalent resistance value Rload (Vitelli, 2014). Furthermore, Fig. 19 clearly highlights that dangerous overvoltages can appear at the terminals of the better irradiated sub PV string of the conventional architecture ($V_{0,1\text{-}th}$ in Fig. 19).

5. Conclusions

A battery-based architecture for PV plants endowed with a distributed maximum power tracker has been introduced and discussed. Properly designed and distributed battery-packs together with very simple boost-type DC/DC converters have been used to optimise both power generation and availability of the PV plant, also in presence of criticality in the PV field and/or in the grid operating conditions. Emphasis has been dedicated on how choosing the rated voltage of batteries while only a little attention has been dedicated to the choice and management of their capacity value, because this last strictly depends from the specific scenario of solar irradiance criticality that has to be coped with; as a consequence, additional issues directly related to the capacity of batteries (e.g. additional costs) have not been investigated at this stage. Once the rated voltage of batteries has been properly matched with operating characteristics of PV modules, DC/DC converters can be additionally operated with any available MPPT algorithm and the PV generation of the maximum power is always guaranteed both under balanced and/or unbalanced PV field exposure to the atmospheric agents and for any external grid operating conditions. Differently from conventional PV plants with DMMPT but with no batteries, a central MPPT function proved not to be strictly necessary; furthermore, thanks to the energy storage presence, power injected on the distribution grids by the central inverter can be controlled both by the grid Operator (to contain problems on the grids without frustrating the MPPT function) or by its owner (i.e. for controlling the SOC and for avoiding overcharge and undercharge of batteries for maximising their performances and lifetime). Measurements on a small-power lab prototype together with Pspice numerical simulations on a 3 kWp case-study have been operated and, differently from conventional DMPPT, no overvoltages on sensitive circuitry components (i.e. power switches and capacitors) have been registered, either under ordinary conditions (i.e. balanced irradiance conditions) or under extraordinary conditions (i.e. in presence of significant mismatches among sub PV strings of a PV field).

References

Ali, S.M., Pattanayak, Punyashree, Sanki, Prasun, Sabat, R.R., 2012. Modeling and control of grid-connected hybrid photovoltaic distributed generation system. Int. J. Eng. Sci. Emerg. Technol. 4 (1), 125–132, December 2012. ISSN: 2231–6604 IJESET.

Alonso, R., Roman, E., Sanz, A., Santos, V.E.M., Ibanez, P., 2012. Analysis of inverter-voltage influence on distributed MPPT architecture performance. IEEE Trans. Ind. Electron. 59 (10), 3900–3907

Beltran, H., Bilbao, E., Belenguer, E., Etxeberria-Otadui, I., Rodriguez, P., 2013. Evaluation of storage energy requirements for constant production in PV power plants. IEEE Trans. Ind. Electron. 60 (3), 1225–1234.

Bong-Yeon, Choi, Yong-Su, Noh, Young-Hyok, Ji, Byoung-Kuk, Lee, Chung-Yuen, Won, 2012. Battery-Integrated power optimizer for PV battery hybrid power generation system. In: IEEE Vehicle Power and Propulsion Conference, October 9–12, 2012, Seoul, Korea, pp. 1343– 1348.

Burgio, A., Carbone, R., Morello, R., Pinnarelli, A., 2013. Grid-connected PV plants based on a distributed energy-storage system and a multilevel inverter. Int. Rev. Electr. Eng. (IREE) 8 (4), 1267–1278, ISSN: 1827-6660.

Carbone, R., 2009a. Grid-connected photovoltaic systems with energy storage. IEEE International Conference on Clean Electrical Power, 2009. Capri, Italy, June 2009.

Carbone, R., 2009b. A passive MPPT technique for grid-connected photovoltaic systems. In: 20-th International Conference and Exhibition on Electricity Distribution – Part 1. CIRED 2009. Prague.

Carbone, R., 2010. In: Sheikh, Rafiqul Islam (Ed.), Energy Storage in Grid-Connected Photovoltaic Plants. INTECH Open Access Publisher, Chapter 4 of the Book ‘‘Energy-Storage”, ISBN 978-953-307- 119-0, 2010.

Carbone, R., 2011. In: Carbone, Rosario (Ed.), Energy Storage in the Emerging Era of Smart Grids. INTECH Open Access Publisher, p. 492, ISBN 978-953-307-269-2, September 22, 2011. DOI: 10.5772/737.

Carbone, R., Tomaselli, A., 2012. Numerical analysis of quality of power generated by an innovative AC PV module with onboard energy storage. In: Proceedings of the 12th WSEAS International Conference on Electric Power Systems, High Voltages, Electric Machines (POWER ’12). Prague, Czech Republic, September 24–26, 2012. ISBN: 978-1-61804-128-9.

Carbone, R., Carotenuto, R., Della Corte, F.G., Felini, C., Iero, D., Merenda, M., Pangallo, G., 2014. SPICE modelling of a complete photovoltaic system including modules, energy storage elements and a multilevel inverter. Elsevier Sol. Energy 107 (September), 338–350.

Castaner, Luis, Silvestre, Santiago, 2002. Modelling Photovoltaic Systems Using Pspice. John Wiley & Sons Ltd, The Atrium, Southern Gate, Chichester, West Sussex PO19 8SQ, England, ISBN: 978-0-470-84527-1.

Castaner, Luis, Aloy, Raimond, Carles, Daniel, 1995. Photovoltaic system simulation using a standard electronic circuit simulator. Prog. Photovol.: Res. Appl. 3 (4), 239–252. http://dx.doi.org/10.1002/pip.4670030405.

CEI 0-16, 2012: Reference Technical Rules for the Connection of Active and Passive Consumers to the HV and MV Electrical Networks of Distribution Company.

CEI 0-21, 2014: Reference Technical Rules for the Connection of Active and Passive Users to the LV Electrical Utilities.

Chen, Cheng-Wei, Chen, Kun-Hung, Chen, Yaow-Ming, 2014. Modeling and controller design of an autonomous PV module for DMPPT PV systems. IEEE Trans. Power Electron. 29 (9), 4723–4732.

Deline, C., Marion, B., Granata, J., Gonzalez, S., 2011. A performance and economic analysis of distributed power electronics in photovoltaic systems. Technical Report NREL/TP-5200-50003, January 2011.

Du, Yang, Lu, Dylan Dah-Chuan, 2011. Battery-integrated boost converter utilizing distributed MPPT configuration for photovoltaic systems. Sol. Energy 85, 1992–2002, ELSEVIER.

Edrington, C.S., Balathandayuthapani, S., Jianwu Cao, 2010. Analysis of integrated storage and grid interfaced photovoltaic system via nineswitch three-level inverter. In: IEEE Industrial Electronics Society Annual Conference IECON 2010 – 36th, pp. 3258–3262. ENTSO-E Network Codes.

Femia, N., Lisi, G., Petrone, G., Spagnuolo, G., Vitelli, M., 2008. Distributed maximum power point tracking of photovoltaic arrays: novel approach and system analysis. IEEE Trans. Ind. Electron. 55 (7), 2610–2621.

IEEE 1547-2003. Standard for Interconnecting Distributed Resources with Electric Power Systems.

IEEE 1547.3-2007 Standard: Guide for Monitoring, Information Exchange, and Control of Distributed Resources Interconnected with Electric Power Systems.

Jabalameli, N., Masoum, M.A.S., Shahnia, F., Mehr, T.H., 2013. Impact of battery rating on performance of rooftop PV supporting household loads, regulating PCC voltage and providing constant output power to grid. In: Power Engineering Conference (AUPEC), 2013 Australasian Universities, pp. 1–6.

Kim, Hongrae, Parkhideh, B., Bongers, T.D., Gao, Heng, 2013. Reconfigurable solar converter: a single-stage power conversion PV battery system. IEEE Trans. Power Electron. 28 (8), 3788–3797.

Patel, H., Agarwal, V., 2008. Maximum power point tracking scheme for PV systems operating under partially shaded conditions‘‘. IEEE Trans. Ind. Electron. 55 (4), 1689–1698.

Poshtkouhi, S., Palaniappan, V., Fard, M., Trescases, O., 2011. A general approach for quantifying the benefit of distributed power electronics for fine grained MPPT in photovoltaic applications using 3D modeling. IEEE Trans. Power Electron. 27 (11), 4656–4666.

Ramos-Paja, C.A., Saavedra-Montes, A.J., Vitelli, M., 2013. Distributed maximum power point tracking with overvoltage protection for PV systems. Dyna 80 (178), 141–150, Medellin, April 2013. ISSN 0012- 7353.

Regulation (EC) No 714/2009 of the European parliament, 2009. On Conditions for Access to the Network for Cross-Border Exchanges in Electricity and Repealing Regulation (EC) N. 1228/2003.

Shimizu, T., Hashimoto, O., Kimura, G., 2003. A novel high-performance utility–interactive photovoltaic inverter system. IEEE Trans. Power Electron. 18 (2).

Shmilovitz, Doron, Levron, Yoash, 2012. Distributed maximum power point tracking in photovoltaic systems – emerging architectures and control methods. Automatika 53 (2), 142–155, Online ISSN 1848-3380, Print ISSN 0005-1144.

Silvestre, S., Boronat, A., Chouder, A., 2009. Study of bypass diodes configuration on PV modules. Appl. Energy 86 (9), 1632–1640.

Sun, Kai, Zhang, Li, Xing, Yan, Guerrero, J.M., 2011. A distributed control strategy based on DC bus signaling for modular photovoltaic generation systems with battery energy storage. IEEE Trans. Power Electron. 26 (10), 3032–3045.

TERNA, 2005: Code for Transmission, Dispatching, Development and Security of the Grid.; http://www.terna.it:80/default/home_en/electric_system/grid_code.aspx/language/it-IT/Default.aspx

Vitelli, M., 2014. On the necessity of joint adoption of both distributed maximum power point tracking and central maximum power point tracking in PV systems. Appl. Energy 86 (9), 1632–1640, Progress in Photovoltaics: Research and Applications, vol. 22, Wiley- Blackwell, 2014, pp. 283–299

Walker, G., Sernia, P., 2004. Cascaded dc-dc converter connection of photovoltaic modules. IEEE Trans. Power Electron. 19, 1130–1139

Tables

Table 1
Measured and Pspice simulated values of the maximum power, $\mathbf{P}_{gmax}$, generated by the lab PV module, at the irradiance level $\mathbf{G} = 400$ W/m^2, for different PV cell temperatures, $\mathbf{T}_c$, under a non-optimal load ($\mathbf{R}_L$) conditions and at the optimal value of the DC/DC converter duty cycle, $\mathbf{k}$.

$\mathbf{R}_L$ (Ω)	$\mathbf{T}_c$ (°C)	k	$\mathbf{P}_{gmax}$ (W) measured	$\mathbf{P}_{gmax}$ (W) simulated
5	25	0.70	7.9	8.1
	45	0.73	7.6	7.8
	55	0.80	6.8	7.1
3	25	0.70	7.9	8.2
	45	0.76	7.3	7.6
	55	0.78	6.6	7.2

Figures

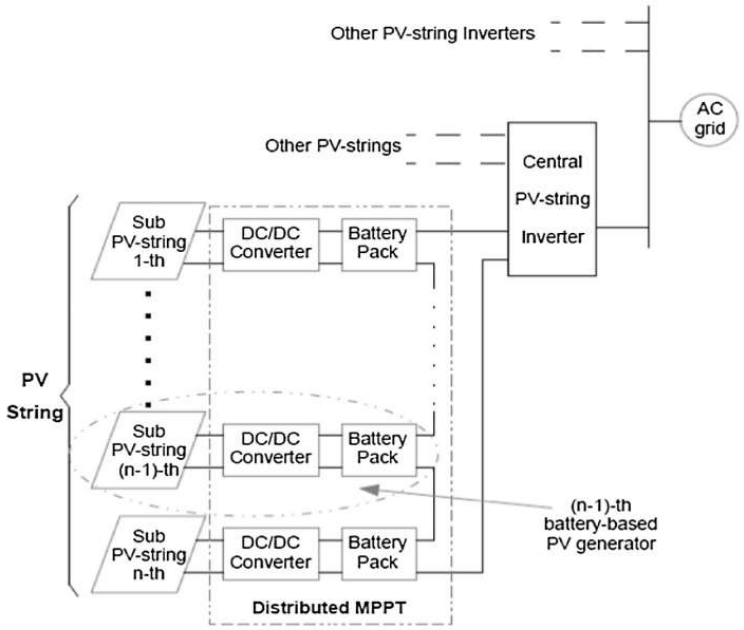

Fig. 1. Architecture of the proposed PV plant with the battery-based distributed MPPT.

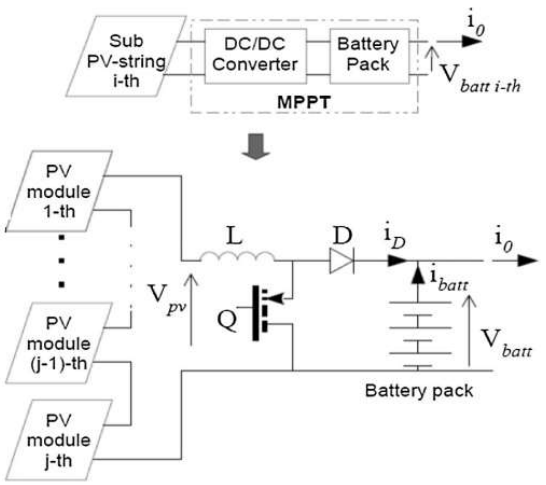

Fig. 2. Electrical scheme of the *i*-th battery-based PV generator with its MPPT.

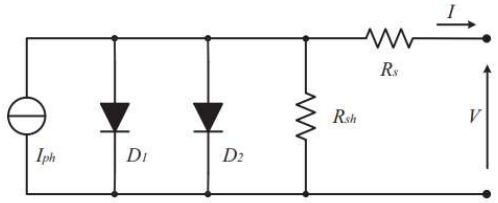

Fig. 3. PV cell equivalent circuit (double-diode exponential model).

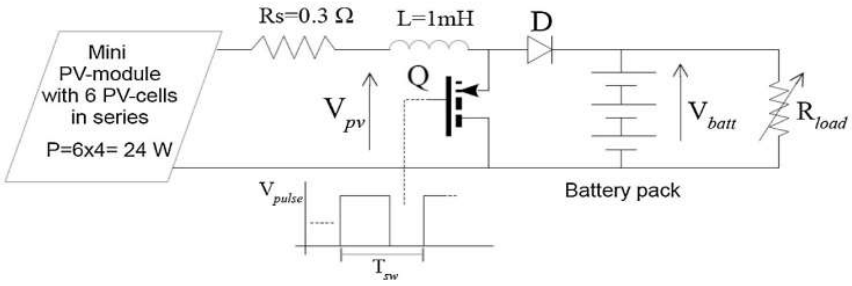

Fig. 4. Electrical scheme of the small-power prototype developed in the laboratory.

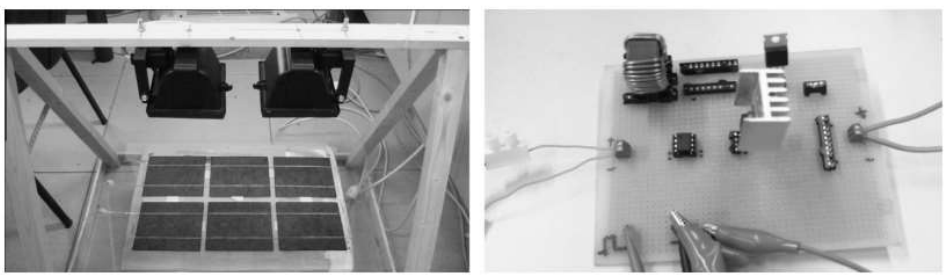

Fig. 5. Some pictures of the small-power prototype developed in the laboratory.

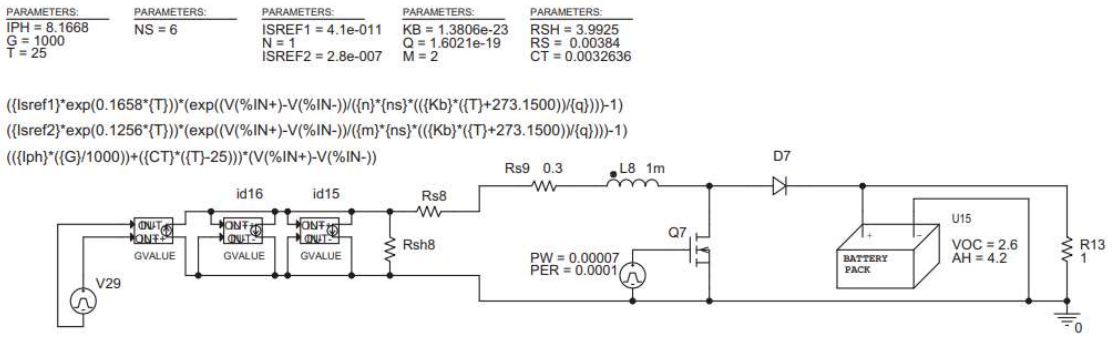

Fig. 6. Pspice circuitry used for simulating the lab prototype.

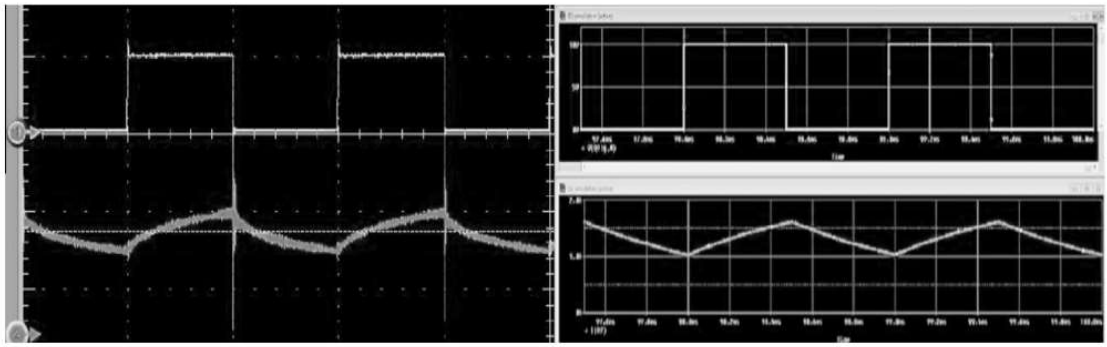

Fig. 7. Measured (left) and simulated (right) waveforms of the Q gating signal and the current generated by the mini PV module at the irradiance level of $\mathbf{G} = 450\ \mathrm{W/m^2}$, a PV cell temperature of $T_c = 45\ ^\circ\mathrm{C}$, $f_{sw} = 1\ \mathrm{kHz}$, duty-cycle = 0.5 and for a non-optimal load condition (5 Ω).

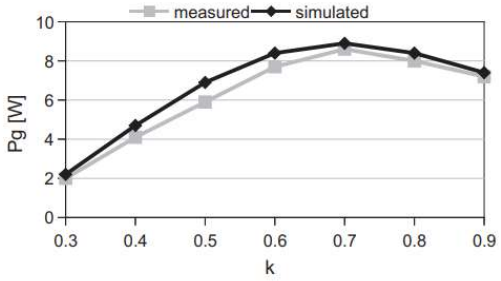

Fig. 8. Power, P_g, generated by the lab PV module at the irradiance level $G = 450\ \mathrm{W/m^2}$, PV cell temperature $T_c = 25\ ^\circ\mathrm{C}$, $f_{sw} = 1\ \mathrm{kHz}$ and for a non-optimal load condition (5 Ω), versus the value of the DC/DC converter duty cycle, k.

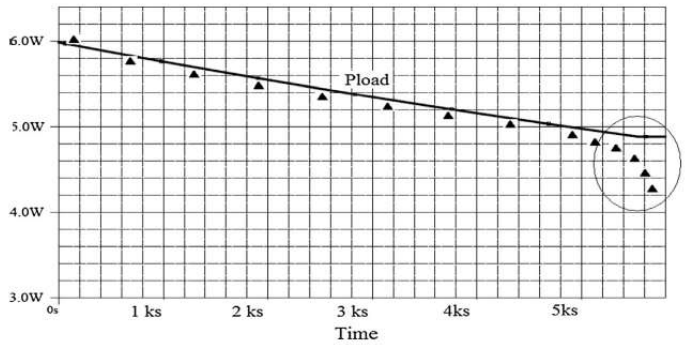

Fig. 9. Simulated (continuous line) and measured (▲) load power, P_{load}, obtained by using a battery-pack with 2.6 V_{oc} and 4.2 A h, during a very long time outage of PV generation at a medium load condition (RL = 0.76 W).

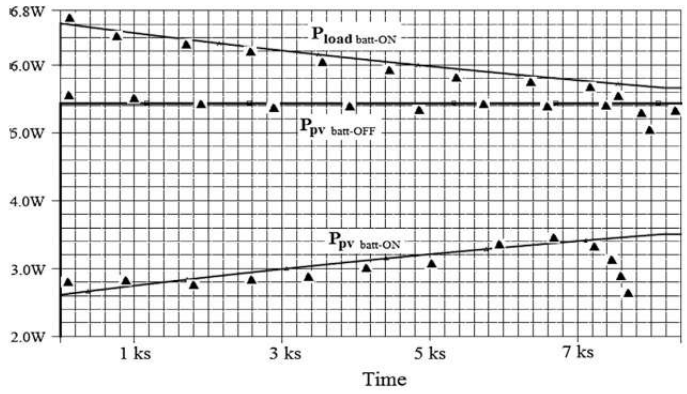

Fig. 10. Simulated (continuous line) and measured (▲) powers: generated by the PV-module with the battery pack switched-OFF, Ppvbatt-OFF, generated by the PV module with the battery-pack (2.6 V_{oc} and 4.2 A h) ON, Ppvbatt-ON, and load power with the battery ON, Ploadbatt-ON, at 280 W/m^2 irradiance level and optimal load (R_L = 0.76 W).

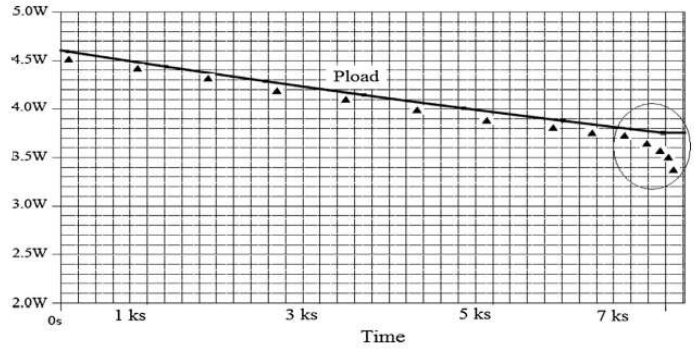

Fig. 11. Simulated (continuous line) and measured (▲) load power, P_{load}, using a battery-pack with 1.37 V_{oc} and 8.4 A h, during a very long time outage of PV generation at medium load condition (R_L = 0.23 W).

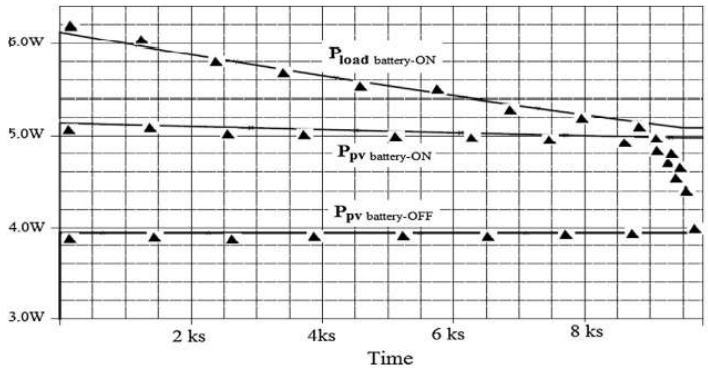

Fig. 12. Simulated (continuous line) and measured (▲) powers: generated by the PV-module with the battery pack switched-OFF, Ppvbatt-OFF, generated by the PV module with the battery-pack (1.37 V_{oc} and 8.4 A h) switched-ON, Ppvbatt-ON, and load power with the battery switched-ON, P_{load} batt-ON, at 280 W/m^2 irradiance level and non optimal load ($R_L = 0.2$ W).

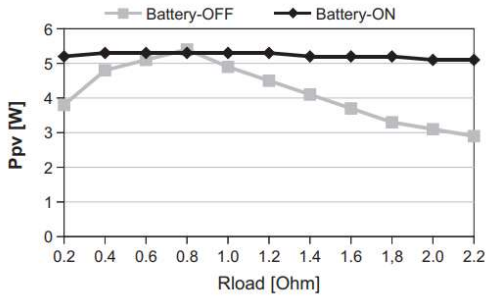

Fig. 13. Power generated by the lab PV-module, Ppv, at the irradiance level of 280 W/m^2 e $T_c = 25$ °C with the battery pack switched-OFF and with the battery pack (1.37 V_{oc} and 8.4 A h) switched-ON, under variable load conditions.

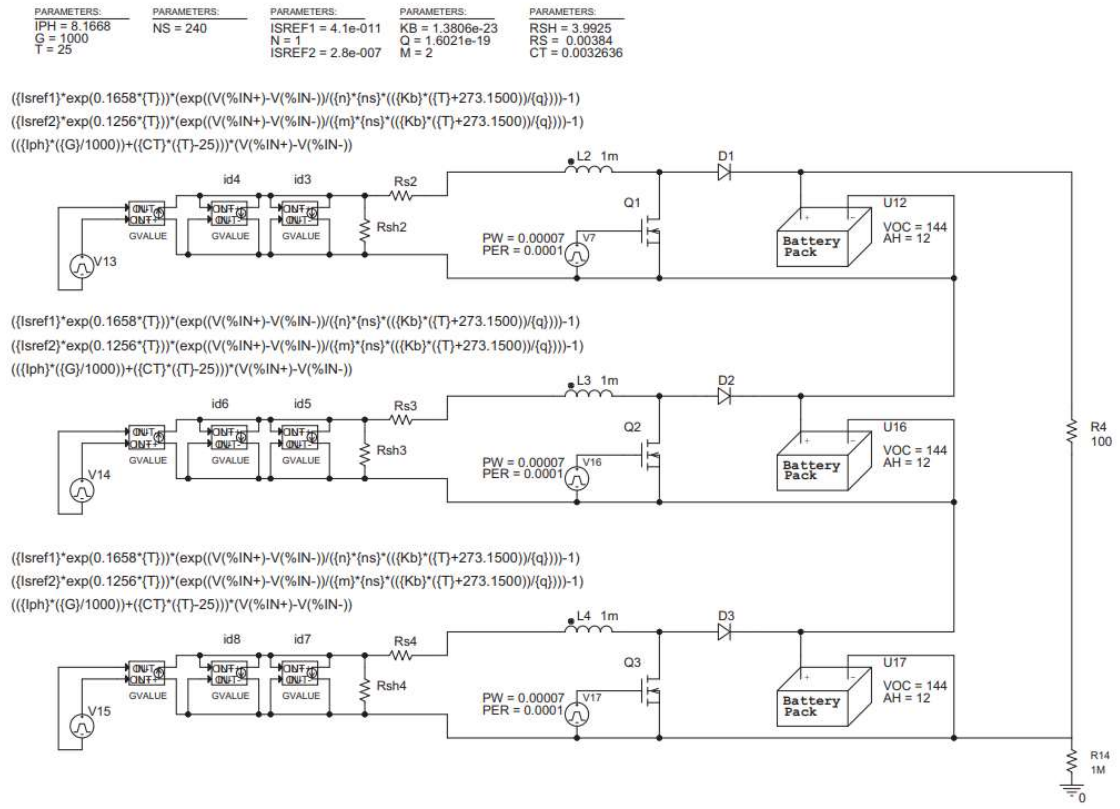

Fig. 14. Pspice circuitry of the architecture proposed for a case-study 3 kWp PV plant.

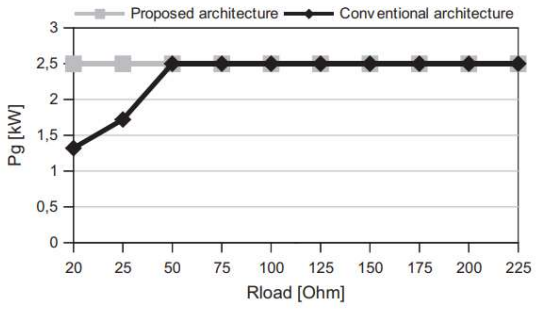

Fig. 15. Maximum power, P_g, generated by the case-study PV plant, under standard conditions (balanced irradiance level **G** = 1000 W/m^2, PV cell temperature $\mathbf{T}_c = 25$ °C), for $\mathbf{f}_{sw} = 10$ kHz and versus non-optimal and variable grid/load operating conditions.

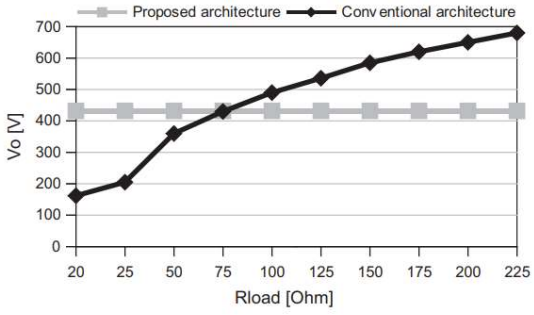

Fig. 16. Output voltage of the whole PV string, $\mathbf{V}_0$, (operating conditions are specified in Fig. 15).

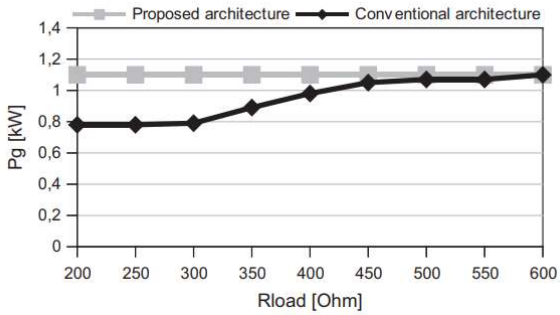

Fig. 17. Maximum power, P_g, generated by the case-study PV plant, under standard PV cell temperature $\mathbf{T}_c = 25\ °C$, $\mathbf{f}_{sw} = 10\ kHz$, irradiance level of $\mathbf{G} = 1000\ W/m^2$ for the sub PV string 1 and irradiance level of $\mathbf{G} = 200\ W/m^2$ for the sub PV strings 2 and 3, under non-optimal and variable load/network conditions.

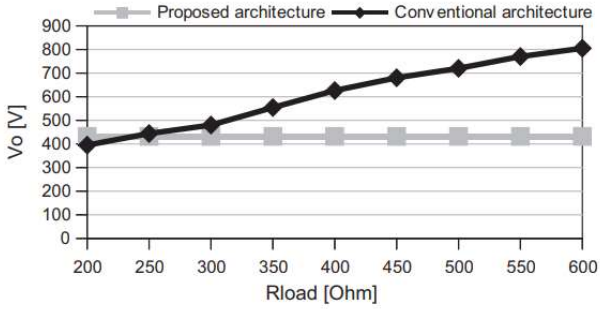

Fig. 18. Output voltages of the case-study PV plant, $\mathbf{V}_0$ (operating conditions are specified in Fig. 17).

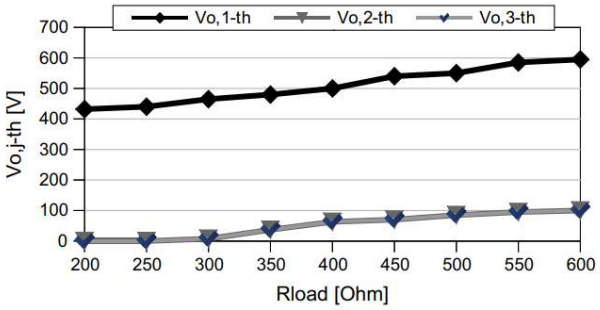

Fig. 19. Output voltages of each sub PV string, $\mathbf{V}_{0,j\text{-th}}$, of the conventional architecture (operating conditions are specified in Fig. 17).